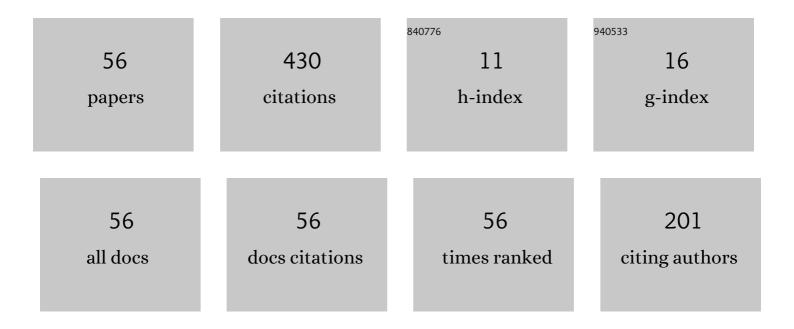


List of Publications by Year in descending order

Source: https://exaly.com/author-pdf/7705394/publications.pdf Version: 2024-02-01



| # | Article | IF | CITATIONS |
|----|---|-----|-----------|
| 1 | Theoretical analysis and synthesis of Al4O4C and Al2CO phase in the resin bonded Al-Al2O3 refractory in N2-flowing. Ceramics International, 2018, 44, 1493-1499. | 4.8 | 27 |
| 2 | In situ synthesis mechanism of 15R–SiAlON reinforced Al ₂ O ₃ refractories by Fe–Si liquid phase sintering. Journal of the American Ceramic Society, 2018, 101, 1870-1879. | 3.8 | 26 |
| 3 | New synthetic route to Al4O4C reinforced Al–Al2O3 composite materials. Solid State Sciences, 2015, 46, 33-36. | 3.2 | 24 |
| 4 | Mechanism of active and passive oxidation of reaction-bonded Si3N4-SiC refractories. Ceramics International, 2017, 43, 10720-10725. | 4.8 | 19 |
| 5 | In-situ synthesis of AlON reinforcing phases in resin bonded Al 2 O 3 composite materials. Journal of Alloys and Compounds, 2017, 711, 1-7. | 5.5 | 18 |
| 6 | Silicon nitridation mechanism in reactionâ€bonded Si ₃ N ₄ –SiC and Si ₃ N ₄ â€bonded ferrosilicon nitride. Journal of the American Ceramic Society, 2018, 101, 4350-4356. | 3.8 | 17 |
| 7 | Study on phase evolution of the resin bonded Al-Al2O3 composites in N2-flowing at high temperature. Journal of Alloys and Compounds, 2019, 784, 1145-1152. | 5.5 | 17 |
| 8 | Controllable preparation and synthetic mechanism of mullite from the bauxite with Fe-rich oxide content. Materials Chemistry and Physics, 2017, 202, 245-250. | 4.0 | 14 |
| 9 | Formation mechanism of elongated β–Si3N4 crystals in Fe–Si3N4 composite via flash combustion. Ceramics International, 2018, 44, 9395-9400. | 4.8 | 13 |
| 10 | Investigation on a postmortem resin-bonded Al-Si-Al2O3 sliding gate with functional gradient feature. Ceramics International, 2018, 44, 6384-6389. | 4.8 | 13 |
| 11 | Novel iron-rich mullite solid solution synthesis using fused-silica and α-Al2O3 powders. Ceramics International, 2019, 45, 4680-4684. | 4.8 | 12 |
| 12 | In situ reaction mechanism of MgAlON in Al–Al2O3–MgO composites at 1700°C under flowing N2. International Journal of Minerals, Metallurgy and Materials, 2017, 24, 1061-1066. | 4.9 | 11 |
| 13 | Formation of (Al ₂ OC) _{1â^'} <i>_x</i> (AlN) <i>_x</i> solid solution starting from Al–Si–Al ₂ O ₃ powder matrix at 1300°C in flowing nitrogen. Journal of the American Ceramic Society, 2019, 102, 6349-6356. | 3.8 | 11 |
| 14 | Reaction bonding alumina with AlN–SiC solid solution by nitridation of matrix containing Al–Si powders. Journal of Materials Science, 2019, 54, 14654-14665. | 3.7 | 10 |
| 15 | Preparation and ladle slag resistance mechanism of MgAlON bonded Al2O3 -MgAlON-Zr2Al3C4-(Al2CO)1-(AlN) refractories. Ceramics International, 2019, 45, 346-353. | 4.8 | 10 |
| 16 | Formation mechanism of Ti(C, N) solid solution in Al-brown fused alumina refractory at 1973 K in flowing N2. Ceramics International, 2020, 46, 2654-2660. | 4.8 | 10 |
| 17 | Effect of Al addition on creep resistance of MgO-Al2O3 composite for sliding plate at 1400 °C. Ceramics International, 2017, 43, 11610-11615. | 4.8 | 9 |
| 18 | Reaction mechanism for in-situ β-SiAlON formation in Fe3Si–Si3N4–Al2O3 composites. International Journal of Minerals, Metallurgy and Materials, 2017, 24, 324-331. | 4.9 | 9 |

| # | Article | IF | CITATIONS |
|----|---|--------------------------------|--------------------|
| 19 | Phase evolution mechanism of nonâ€oxide bonded Al–Al ₂ O ₃ –MgO–ZrO ₂ composites at 1873ÂK in flowing nitrogen. Journal of the American Ceramic Society, 2018, 101, 2162-2169. | 3.8 | 9 |
| 20 | Kinetic study on the anisotropic grain growth of elongated iron-containing mullite. Ceramics International, 2019, 45, 12934-12941. | 4.8 | 9 |
| 21 | In-situ synthesis and reaction mechanism of MgAlON in Al2O3-MgO composites produced in flowing nitrogen. Ceramics International, 2017, 43, 14791-14797. | 4.8 | 8 |
| 22 | Preparation, growth mechanism and slag resistance behavior of ternary Ca 2 Mg 2 Al 28 O 46 (C 2 M 2 A) Tj ETQo | q0.0,0 rgB ⁻ 2.1 | ∏ ¦Overlock ∶ 8 |

| 23 | Role of the vapour phases in the formation mechanism of 15R-SiAlON in FexSiy-Si3N4-Al2O3 composites at 1800â€Â°C. Ceramics International, 2018, 44, 23239-23247. | 4.8 | 7 |
|----|--|------------|---|
| 24 | Controllable synthesis of Al2OC-AlN solid solution by two-step sintering in resin-bonded Al-Al2O3 composites. Materials Chemistry and Physics, 2020, 241, 122410. | 4.0 | 7 |
| 25 | Reaction mechanisms between slag and Ti(C,N)–MgAl2O3–Al2O3 refractories at 1600 °C. Ceramics International, 2020, 46, 27774-27782. | 4.8 | 7 |
| 26 | Formation mechanism of whiskers in Al–MgAl2O4–MgO refractories at 1400°C under N2 atmosphere. Ceramics International, 2020, 46, 20724-20731. | 4.8 | 7 |
| 27 | Novel process for synthesizing fused mullite from titanium-rich medium/low grade or waste bauxite. Ceramics International, 2022, 48, 8228-8234. | 4.8 | 7 |
| 28 | Wear mechanism of a novel Al Si MgAl2O4Al2O3 composite used in the low vessel of an RH secondary refining furnace. Ceramics International, 2019, 45, 11275-11280. | 4.8 | 6 |
| 29 | Combined effect of Fe-Si alloys and carbon on Si3N4 stability at elevated temperatures. Ceramics International, 2019, 45, 3290-3296. | 4.8 | 6 |
| 30 | Study on the synthesis and formation mechanism of Al2OC-AlN solid solution in Al–Al2O3 composite material in air at 1500°C. Solid State Sciences, 2020, 100, 106112. | 3.2 | 6 |
| 31 | Creep behaviour of an Al–Si–Al2O3 composite based on phase evolution at 1300oC. Ceramics International, 2022, 48, 2337-2344. | 4.8 | 6 |
| 32 | Formation mechanism of dense anti-oxidation layer in Al-Si-MgO composites sintered in air condition. Ceramics International, 2018, 44, 3987-3992. | 4.8 | 5 |
| 33 | Formation of dense non-oxide layer in Al–TiO2–MgO–Al2O3 refractories at 1873â€ ⁻ K in flowing N2. Ceramics International, 2019, 45, 19297-19306. | 4.8 | 5 |
| 34 | Investigation of the oxidation mechanism of an Al–Si–Al2O3 composite at 1100°C and 1550°C. Ceram International, 2020, 46, 13813-13820. | ics 4.8 | 5 |
| 35 | Cost-effective manufacture and synthesis mechanism of ferrosilicon nitride porous ceramic with interlocking structure. Ceramics International, 2021, 47, 5265-5272. | 4.8 | 5 |
| 36 | One step sintering of homogenized bauxite raw material and kinetic study. International Journal of Minerals, Metallurgy and Materials, 2016, 23, 1231-1238. | 4.9 | 4 |

22

Yon

| # | Article | IF | CITATIONS |
|----|---|-----|-----------|
| 37 | Formation mechanism of Sialon in alumina-ferro-silicon-nitride composite under nitrogen atmosphere at high temperatures. Solid State Sciences, 2018, 86, 19-23. | 3.2 | 4 |
| 38 | Study on formation mechanism and morphology evolution of Iron-exsolution mullite. Materials Letters, 2019, 246, 9-12. | 2.6 | 4 |
| 39 | Formation mechanism and controllable preparation of Ti(C,N) in Al–TiO2–Al2O3 composite at 1673â€ [–] K in flowing N2. Materials Chemistry and Physics, 2020, 239, 122128. | 4.0 | 4 |
| 40 | Formation mechanism of γ-AlON and β-SiC reinforcements in a phenolic resin-bonded Al–Si–Al2O3 composite at 1700°C in flowing N2. Journal of Materials Science, 2020, 55, 5772-5781. | 3.7 | 4 |
| 41 | Fracture behavior and microstructure analysis of Al2O3–MgO–CaO castables for steel-ladle purging plugs. International Journal of Minerals, Metallurgy and Materials, 2016, 23, 1333-1339. | 4.9 | 3 |
| 42 | Performance investigation of resin bonded ferro-silicon nitride-corundum refractories after creep at 1300 °C. Ceramics International, 2017, 43, 16424-16429. | 4.8 | 3 |
| 43 | Synthesis of (Al ₂ OC) _x (AlN) _{1-x} whiskers via Al ₂ O(g) transient phase in Al-Al ₂ O ₃ composite at 1000–1300°C in flowing N ₂ . Journal of Asian Ceramic Societies, 2020, 8, 624-633. | 2.3 | 3 |
| 44 | Effect of Si3N4 mesophase on the formation of Al2OC-AlNss in resin-bonded Al–Al2O3 composites. Ceramics International, 2021, 47, 25491-25496. | 4.8 | 3 |
| 45 | In situ formation mechanism of spinel-like Al5O6N and plate-like Al7O3N5 in the two-step sintered Al–Al2O3 composites. Materials Chemistry and Physics, 2021, 271, 124951. | 4.0 | 3 |
| 46 | Thermodynamic analysis of Al O (g) and phase and micro-structure evolution of the resin bonded Al–Al2O3–ZrO2 refractories under air embedded in coke breeze. Journal of Alloys and Compounds, 2021, 855, 157216. | 5.5 | 2 |
| 47 | Phase composition, microstructure, and properties of Al4O4C–(Al2OC)1-(AlN) –Zr2Al3C4–Al2O3 refractories prepared at high temperatures in nitrogen. Ceramics International, 2021, 47, 30298-30309. | 4.8 | 2 |
| 48 | Phase evolution of a novel silicon-alumina-fused mullite-containing Ti2O3 refractory at 1300°C in N2. Ceramics International, 2022, 48, 31686-31694. | 4.8 | 2 |
| 49 | Enhanced properties of MgO–Al 2 O 3 composite materials with Al powder addition under 1300°C creep test and its mechanism analysis. Solid State Sciences, 2017, 66, 38-43. | 3.2 | 1 |
| 50 | Novelty phase synthesis mechanism and morphology in resin-bonded Al-Al2O3-TiO2 composites at high temperatures under flowing N2. International Journal of Minerals, Metallurgy and Materials, 2019, 26, 1177-1185. | 4.9 | 1 |
| 51 | Oxidation mechanism of Al-TiO2-MgO-Al2O3 composites after the treatment at 1500°C in N2-blowing. Materials Chemistry and Physics, 2020, 248, 122937. | 4.0 | 1 |
| 52 | Effect of TiO2 on the formation of novel non-oxide phases in Al–MgO–Al2O3 composite at high temperatures in flowing N2. Materials Chemistry and Physics, 2021, 258, 123963. | 4.0 | 1 |
| 53 | Inâ€situ synthesis of 15Râ€Sialon from Alâ€Si ₃ N ₄ â€Al ₂ O ₃ composite at 1500°C via liquidâ€phase sintering. Journal of the American Ceramic Society, 2022, 105, 2268-2276. | 3.8 | 1 |
| 54 | Performance of silica bricks with ferrosilicon nitride as the mineralizer. Ceramics International, 2022, 48, 26791-26799. | 4.8 | 1 |

Yon

| # | Article | IF | CITATIONS |
|----|---|-----|-----------|
| 55 | A novel dense Al ₂ O ₃ -Ti ₂ O ₃ slag synthesized while ferro-titanium alloy making. Journal of Asian Ceramic Societies, 2022, 10, 150-157. | 2.3 | Ο |
| 56 | Properties of both Chinese silica brick and silica raw material. Ironmaking and Steelmaking, 0, , 1-11. | 2.1 | 0 |